Composites Part B 175 (2019) 107189

Contents lists available at ScienceDirect

Composites Part B

journal homepage: www.elsevier.com/locate/compositesb

Cu(0) and Cu(II) decorated graphene hybrid on improving fireproof efficiency of intumescent flame-retardant epoxy resins

Tao-Ping Ye [a], Shi-Fu Liao [b], Yi Zhang [c], Ming-Jun Chen [a,*], Yao Xiao [a], Xing-Ya Liu [a], Zhi-Guo Liu [a], De-Yi Wang [a,d,**]

[a] School of Science, Xihua University, Chengdu, 610039, China
[b] Guangdong Shunde Tongcheng New Materials Technology Co.Ltd, Foshan, 528333, China
[c] Sichuan Fire Research Institute of Ministry of Public Security, Chendu, 610036, China
[d] IMDEA Materials Institute, C/Eric Kandel, 2, Getafe, Madrid, 28906, Spain

ARTICLE INFO

Keywords:
Hybrid
Synergism
Epoxy resin
Flame retardancy
Smoke suppression

ABSTRACT

To explore the synergism and mechnism of diverse forms of copper-decorated graphene on improving the fireproof efficiency of ammonium polyphosphate (APP) based polyamide-cured epoxy resin (EP), Cu(0) and Cu(II) decorated graphene hybrids (Cu^{2+}-GO, Cu-rGO and CuO-GNS) were prepared through facile methods and used as synergists in EP/APP system. Cu^{2+}-GO exhibits better synergistic effect with APP than Cu-rGO and CuO-GNS on reducing heat release of EP. Because Cu^{2+} is easier than Cu and CuO to go through various oxidation states and intermediates, which catalyze EP/APP system rapid formation of protective char layer containing crosslinked junctions of P (V) organic phosphates and Cu (II) salts. CuO-GNS exhibits better smoke suppression and harmful gases reduction in EP/APP matrix, such as aliphatic hydrocarbons, aromatic compounds and CO, due to its better conversion of CO to CO_2 through a redox cycle. This work provides a promising strategy for preparation of EP with excellent flame retardancy and smoke suppression at low addition.

1. Introduction

Epoxy resin (EP) is a highly flammable thermoset [1]. A great deal of toxic fumes, which consists of carbon monoxide, aromatic compounds and aliphatic hydrocarbons, will be concomitantly released during its combustion [2]. Intumescent flame retardant (IFR) technique is the most promising method to endow polymers with flame retardancy and smoke suppression simultaneously on account of its outstanding condensed phase mechanism [3,4]. Ammonium polyphosphate (APP) is a typical flame retardant for building IFR system, for it provides both acid and gas sources [5]. Polyamide-cured EP, which has a large amount of hydroxyl groups, can be used as carbon source for IFR by itself [6,7]. However, the single APP-based polyamide-cured EP composite still exist some defects [8]. For instance, the carbonization rate is not fast enough and the char layer is poor in compactness.

Metal bound compounds have the potential on enhancing flame retardancy and smoke suppression of materials as synergists [9–11]. Copper in diverse forms, such as oxides, salts, complexes and chelates, have been found exceptional activity toward carbon monoxide (CO) oxidation, char formation and heat release reduction. Copper clusters have been proved that it can promote CO oxidation by electron storage and relase, according to the density functional theory calculations [12–14]. Naik and Liu found that copper complexes have positive impact on char formation by the catalytic action of copper ion [15,16]. It was reported that CO can be oxidized to CO_2 with high conversion rate of 99.5% by Cu_2O [17]. In addition, we have found that Cu_2O exhibits excellent synergistic flame-retardant effect in APP-based intumescent EP system, due to the catalytic action of Cu_2O on accelerating char formation rate, improving the amount and compactness of char, as well as promoting the conversion of CO into CO_2 through redox cycle [18,19]. However, Cu_2O has the defects of poor dispersibility, easy settleability and oxidation.

Graphene oxide (GO), an oxidized form of graphene, has excellent solution processability and chemical reactivity due to its abundant oxygen-containing groups (carboxyl, hydroxyl and epoxy groups) [20–22]. In addition, GO is easy to be converted into a more stable form

* Corresponding author.
** Corresponding author. School of Science, Xihua University, Chengdu, 610039, China.
E-mail addresses: cmjchem@126.com (M.-J. Chen), deyi.wang@imdea.org (D.-Y. Wang).

https://doi.org/10.1016/j.compositesb.2019.107189
Received 10 March 2019; Received in revised form 8 July 2019; Accepted 9 July 2019
Available online 10 July 2019
1359-8368/© 2019 Published by Elsevier Ltd.

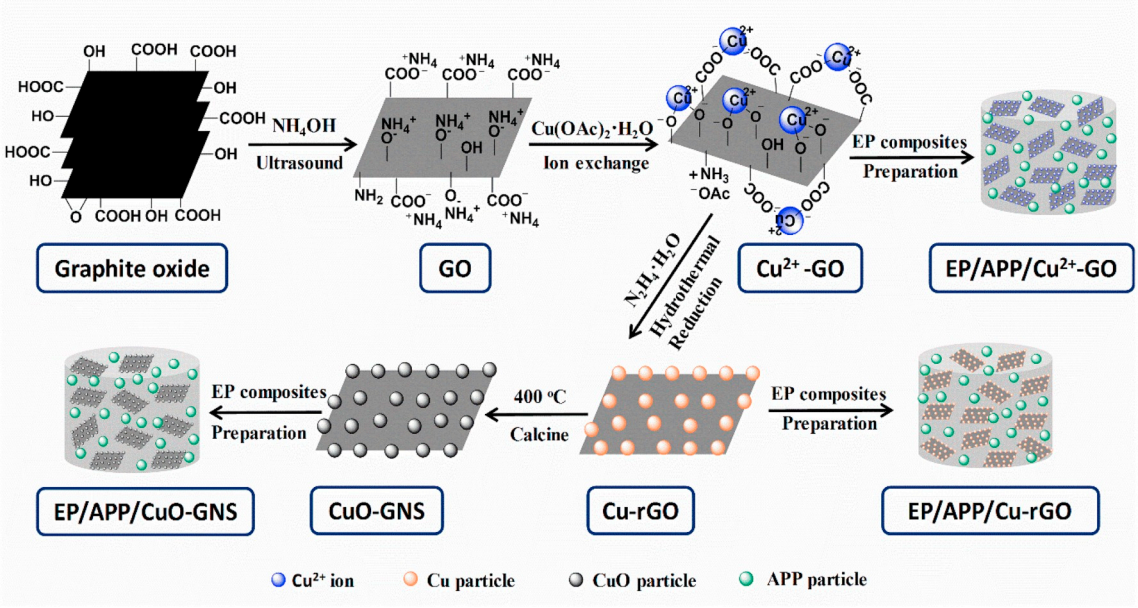

Fig. 1. The preparation process of hybrids (Cu^{2+}-GO, Cu-rGO, CuO-GNS) and its epoxy composites.

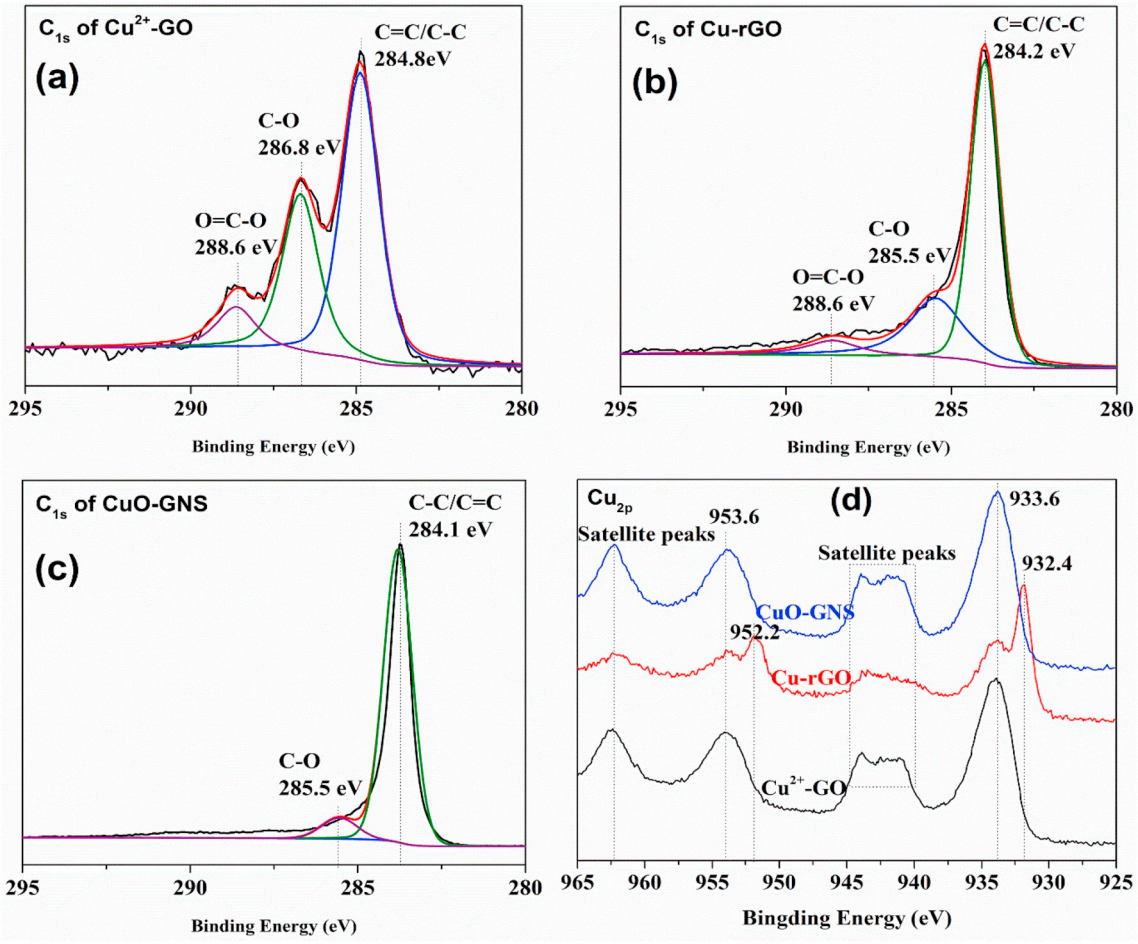

Fig. 2. XPS spectra (C_{1s} and Cu_{2p}) of Cu^{2+}-GO (a, d), Cu-rGO (b, d) and CuO-GNS (c, d).

of reduced GO (rGO). Both of them have a large specific surface area, which makes them become ideal carriers for metal compounds. Interestingly, metal decorated graphene has the advantages of (i) restraining the aggregation of graphene sheets [23–25], (ii) improving the catalytic activity of metal compounds [26,27], (iii) increasing the dispersion and compatibility of graphene and metal compounds in polymer matrixes

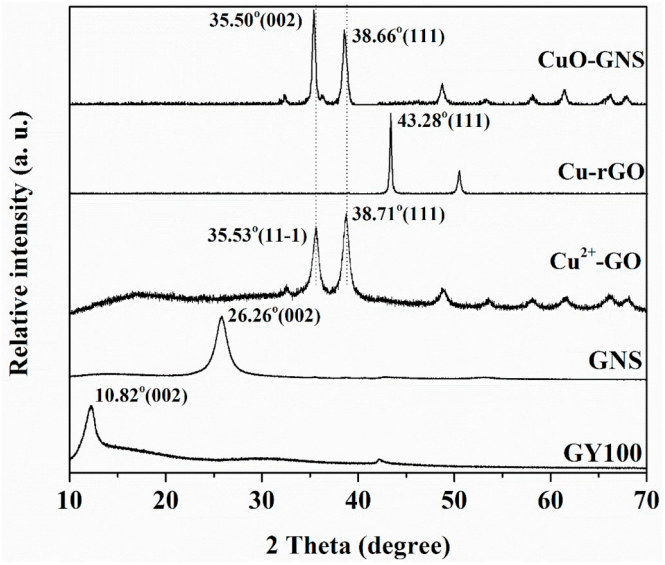

Fig. 3. X-ray diffraction pattern of GO, GNS, Cu^{2+}-GO, Cu-rGO and CuO-GNS.

[28–30]. Therefore, metal oxides attached graphene has good prospects in catalytic and flame-retardant fields, for the physical barrier effect of graphene and the catalytic activity of metal oxides. Especially, copper oxides decorated graphene plays positive catalytic role in CO oxidation and aromatic bond formation [31–34]. However, no systematic study of diverse forms of copper-decorated graphene on how to improve fire-proof efficiency have been undertaken so far.

Therefore, this study was conducted to explore the synergism and mechanism of diverse forms of copper-decorated graphene on improving the flame retardancy and smoke suppression of APP-based EP composite. Herein, Cu(0) and Cu(II) decorated graphene hybrids (Cu^{2+}-GO, Cu-rGO and CuO-GNS) were prepared through facile methods. Then, Cu^{2+}-GO, Cu-rGO and CuO-GNS were incorporated into EP/APP composite and their effects on flame retardancy, smoke and toxic gases reduction, as well as thermal decomposition behavior were investigated. In addition, the gaseous and condensed pyrolysis products were analyzed in detail to explain the flame-retardant and smoke-suppressant mechanisms.

2. Materials and methods

2.1. Materials

Diglycidyl ether of biphenol A (E−44) with epoxy value of 4.4 mol/kg was purchased from Nantong Xingchen Synthetic Material Co. Ltd., China. Commercial polyamide (PA650) was obtained from Xiangtan Hongsang Viscose Materials Co., Ltd., China. Graphite oxide (GY100) with oxygen content of 30% was purchased from Shanghai Xinchi Energy Technology Co., Ltd., China. Copper acetate monohydrate (AR, 99%), ammonia solution (AR, 25%-28%), hydrazine monohydrate (AR, 80%) and alcohol (AR, 99.5%) were purchased from Chengdu Kelong Chemicals Ind. Co., China. Commercial form II ammonium polyphosphate (APP) was supplied by Shifang Taifeng New Flame Retardant Co., Ltd., China. Deionized water was obtained by our laboratory itself. All reagents were used without further purification.

2.2. Preparation of Cu^{2+}-GO, Cu-rGO and CuO-GNS

Graphene oxide (GO) solution was prepared from graphite oxide (GY100) via ultrasonic exfoliating and microwave heating simultaneously. GO contains abundant carboxyl and phenolic hydroxy, which are feasible to react with ammonia, thus the ion exchange reaction between Cu^{2+} and NH_4^+ is achievable. 0.1 g of GY100 was dissolved in 150 mL deionized water with ultrasonication and microwave treatment, and pH was adjusted to 7-8 with ammonia solution. Then, 1.0 g copper acetate monohydrate was added in the solution with vigorous stirring for 1 h at 50 °C. The solution was further stirred overnight under room temperature. Finally, it was separated by suction filtration, the filter cake was washed with 500 mL deionized water each time in beaker until

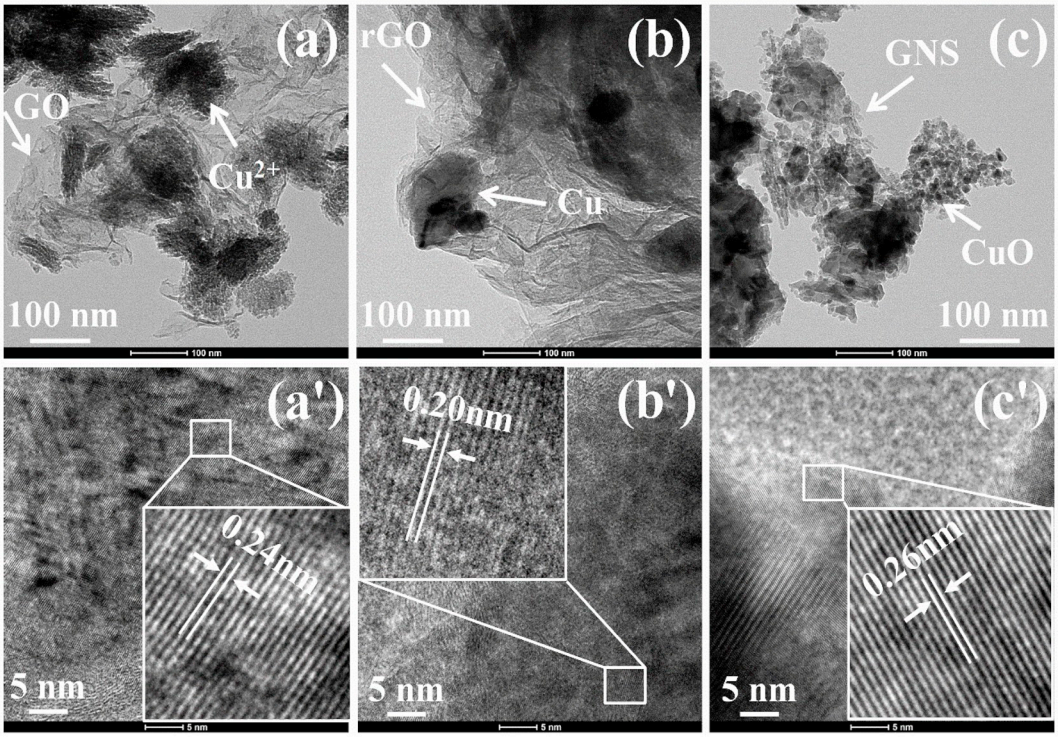

Fig. 4. TEM images of Cu^{2+}-GO (a, a′), Cu-rGO (b, b′) and CuO-GNS (c, c′).

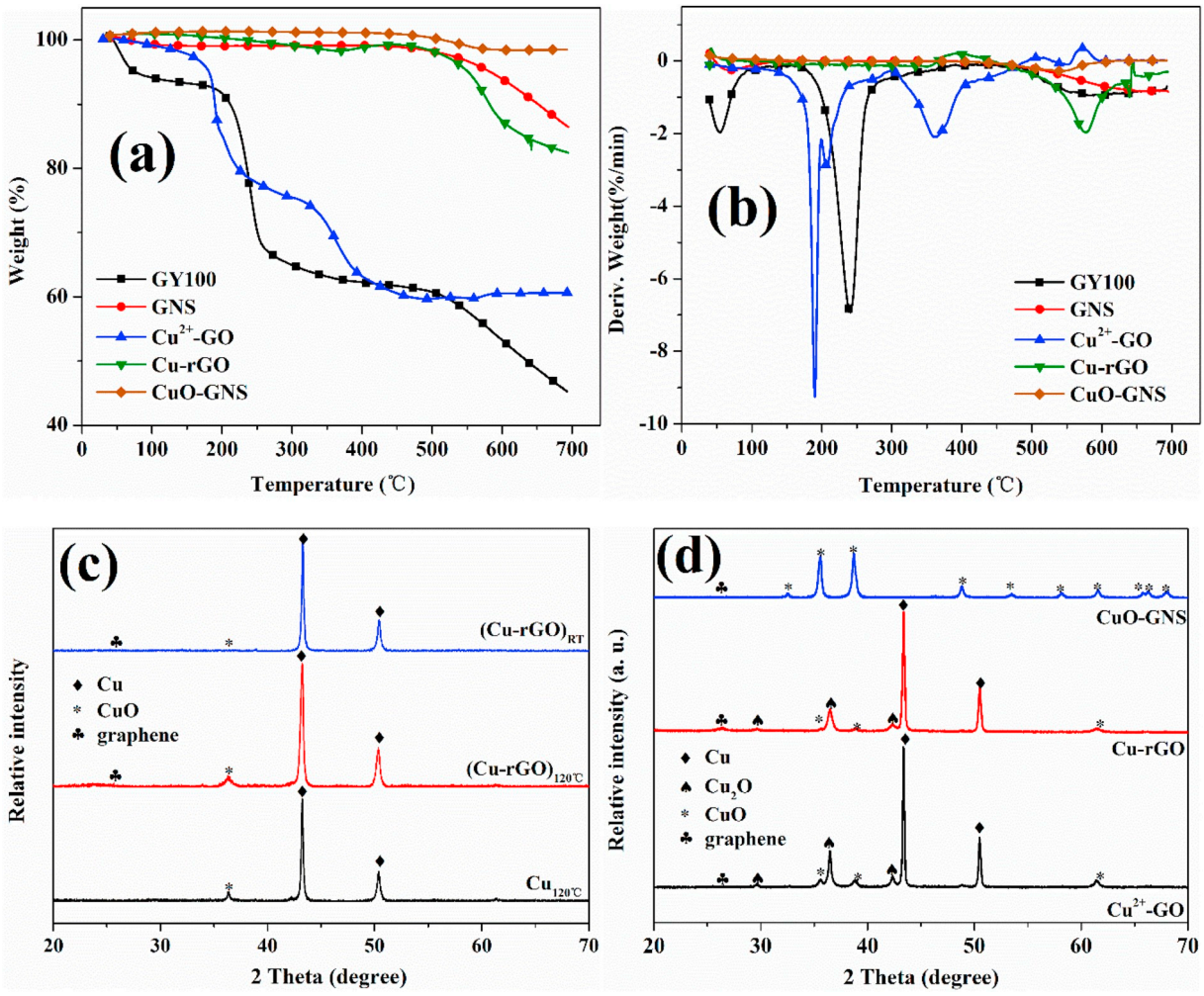

Fig. 5. TG (a), DTG (b) curves of GY100, GNS, Cu^{2+}-GO, Cu-rGO, CuO-GNS and the lattice structures of residues after curing (c) and TGA testing (d).

Table 1
TGA data of GY100, GNS, Cu^{2+}-GO, Cu-rGO and CuO-GNS at the heating rate of 10 °C/min in N_2.[a]

Sample	$T_{5\%}$ (°C)	T_{max1} (°C)	T_{max2} (°C)	wt_R^{700} (%)
GY100	76	55	240	45
GNS	583	659		86
Cu^{2+}-GO	181	190	364	60
Cu-rGO	551	577		82
CuO-GNS		550		98

[a] $T_{5\%}$ denotes the temperature at 5% weight loss; T_{max} denotes the temperature at the maximum weight loss stage; R_{max} represents mass loss rate at T_{max}; wt_R^{700} denotes the weight of char residue at 700 °C.

the filtrate no longer appeared blue. Then, the product was washed 3 times with anhydrous ethanol to ensure that free copper ions were completely removed. The GO coordinated with Cu^{2+} was labeled as Cu^{2+}-GO, which was dried in a vacuum at 60 °C for 6 h.

Then, 0.5 g prepared Cu^{2+}-GO was dissolved in 100 mL deionized water, and 0.5 mL hydrazine monohydrate was added as reductant. The mixture was heated up to 120 °C in a 150 mL hydrothermal reactor and stood for 4 h. Cu decorated reduced graphene oxide (Cu-rGO) was obtained after filtrating, washing and drying in a vacuum at 60 °C for 6 h. The CuO modified graphene nanosheet (CuO-GNS) was obtained by calcining Cu-rGO at muffle furnace for 2 h at 400 °C. Graphene nanosheet (GNS) was prepared at the same process of CuO-GNS without addition of copper acetate monohydrate. The preparation process of

Table 2
The formulations and flammability test (LOI and UL-94) data of epoxy composites.[a].

Sample	E44 (wt%)	PA650 (wt%)	APP (wt%)	SYN (wt%)	UL-94	LOI (%)
Neat EP	55.55	44.44	/	/	NR	20.0 ± 0.5
EP/30%APP	38.89	31.11	30.00	/	V-0	36.5 ± 0.5
EP/29%APP	39.46	31.54	29.00	/	V-1	36.0 ± 0.5
EP/28%APP	40.00	32.00	28.00	/	NR	35.5 ± 0.5
EP/28%APP/ 2%GNS	40.00	32.00	28.00	2.00	V-0	37.5 ± 0.5
EP/28%APP/ 2%Cu^{2+}-GO	38.89	31.11	28.00	2.00	V-0	40.5 ± 0.5
EP/28%APP/ 2%Cu-rGO	38.89	31.11	28.00	2.00	V-0	38.0 ± 0.5
EP/28%APP/ 2%CuO-GNS	38.89	31.11	28.00	2.00	V-0	41.0 ± 0.5
EP/16.80% APP/1.20% Cu^{2+}-GO	45.56	36.44	16.80	1.20	V-0	31.5 ± 0.5
EP/21.47% APP/1.53% Cu-rGO	42.78	34.22	21.47	1.53	V-0	34.0 ± 0.5
EP/20.53% APP/1.47% CuO-GNS	43.33	34.67	20.53	1.47	V-0	36.0 ± 0.5

[a] SYN represents synergist (GNS, Cu^{2+}-GO, Cu-rGO and CuO-GNS), NR means no rating.

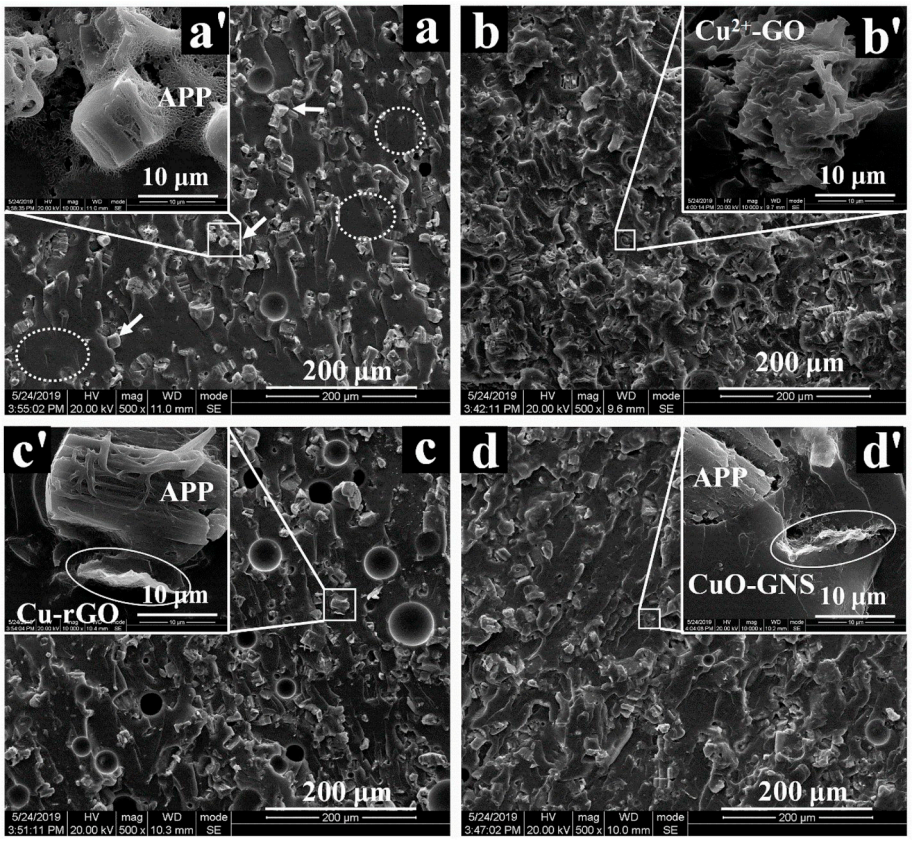

Fig. 6. SEM images of fracture surfaces for EP/28%APP (a, a′), EP/28%APP/2%Cu^{2+}-GO (b, b′), EP/28%APP/2%Cu-rGO (c, c′), and EP/28%APP/2%CuO-GNS (d, d′).

hybrids (Cu^{2+}-GO, Cu-rGO, CuO-GNS) is shown in Fig. 1.

2.3. Preparation of EP composites

EP composites were prepared by mechanical blending and program controlling curing. Typically, E44, PA650 (curing agent), APP (flame retardant) and Cu^{2+}-GO (synergist) were stirred at 70 °C until they were well blended. The mixture was then poured into preheated molds and cured at 80 °C for 2 h and post cured at 120 °C for 2 h. Neat EP and EP composites were prepared via the same procedure, and the formulations are listed in Table 2.

2.4. Measurements

XPS spectra were recorded by a Kratos XSAM80 instrument (U.K.), using Al Kα excitation radiation (hv-1486.6 eV).

X-ray diffraction (XRD) patterns were performed on an X-ray diffractometer (Bruker D8 Ventrue, USA), using Cu Kα radiation ($\lambda = 0.15418$ nm) at 40 kV and 20 Ma with a scanning range from 10 to 70°.

Transmission electron microscope (TEM) micrographs were obtained by a Tecnai G2 F30 (FEI Co., USA) with an acceleration voltage of 300 kV Cu^{2+}-GO, Cu-rGO and CuO-GNS were dispersed in absolute alcohol and then dripped onto copper grids before observation.

Limiting oxygen index (LOI) values was measured at room temperature using a Jiangning JF-3 oxygen index instrument (China) according to ASTM D 2863−97. The size of the specimen was 130 mm × 6.5 mm × 3.2 mm.

The UL-94 vertical burning level was tested on a Jiangning CZF-3 instrument (China) according to ASTM D 3801. The dimension of the sample was 130 mm × 12.7 mm × 3.2 mm.

The flammability of samples was measured by an FTT cone calorimeter instrument (U.K.) under heat flux of 35 kW/m^2 according to ISO 5660−1. The size of specimen was 100 mm × 100 mm × 3 mm.

Thermogravimetric analysis (TGA) was carried out by a Perkin-Elmer STA6000 instrument (UK). The sample (6−8 mg) was heated to 700 °C at a heating rate of 10 °C/min under a dynamic nitrogen flow of 50 mL/min.

The gases evolved during TGA tests were analyzed by coupling TG with FTIR. TGA and FTIR were performed on Perkin-Elmer STA6000 and FRONTIER instrument (UK), respectively. The samples were heated to 700 °C at a heating rate of 10 °C/min under a dynamic nitrogen flow of 50 mL/min.

SEM images were obtained by an INSPECT F scanning electron microscope (US) at the accelerating voltage of 20 kV. The surfaces were coated with a thin gold layer before observation.

3. Results and discussion

3.1. Characterization of hybrids

To find out oxidation states and chemical composition, Cu^{2+}-GO, Cu-rGO and CuO-GNS were measured by XPS. As shown in Fig. 2, the fitting peaks of Cu^{2+}-GO at 284.8 eV, 286.8 eV and 288.6 eV are assigned to C–C/C=C, C–O and O–C=O bonds of C_{1s} spectrum, respectively. It illustrates that GO primarily consists of aromatic rings, hydroxyl and carboxyl groups. Fig. 2 (b) and (c) show that the fitting peaks of C–O and O–C=O for Cu-rGO and CuO-GNS are significantly weakened. This indicates that the oxygen-containing groups were adequately reduced by hydrazine monohydrate. Fig. 2 (d) displays that the Cu_{2p} peaks of both Cu^{2+}-GO and CuO-GNS are assigned to 933.6 eV and 953.6 eV, the Cu_{2p} peaks at 932.4 eV and 952.2 eV belong to Cu-rGO. It confirms that Cu^{2+}-GO and CuO-GNS have the same oxidation state of Cu (II), and Cu-rGO has the oxidation state of Cu (0).

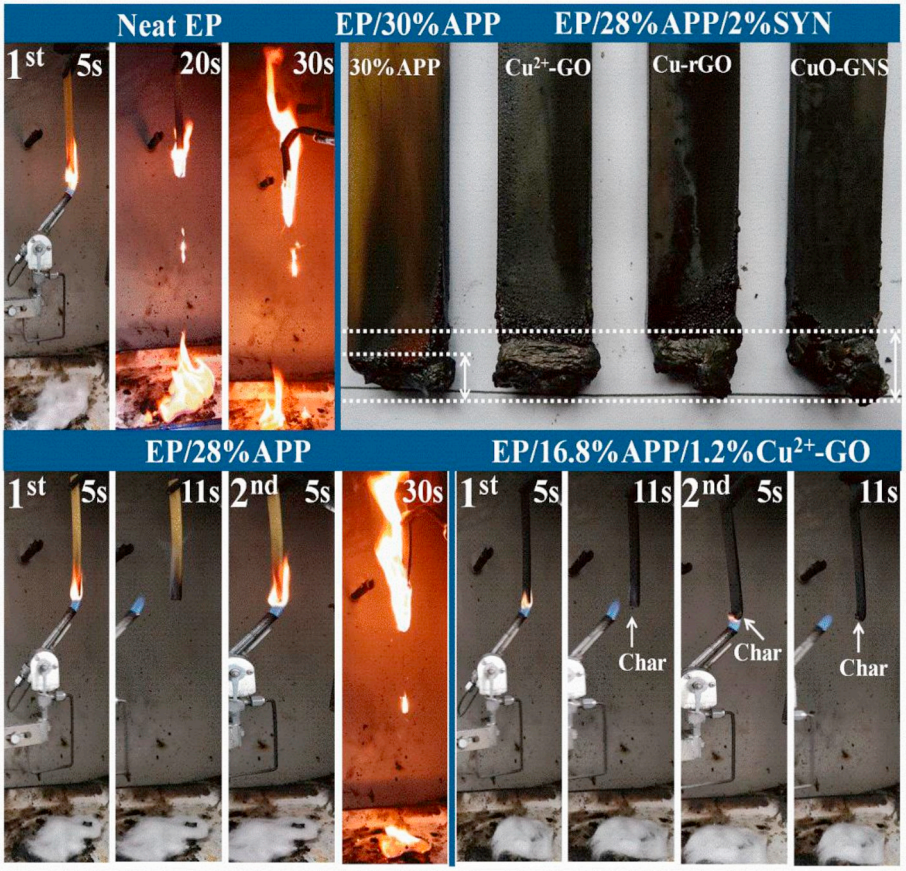

Fig. 7. UL-94 vertical burning test process of neat EP, EP/APP and EP/APP/SYN composites.

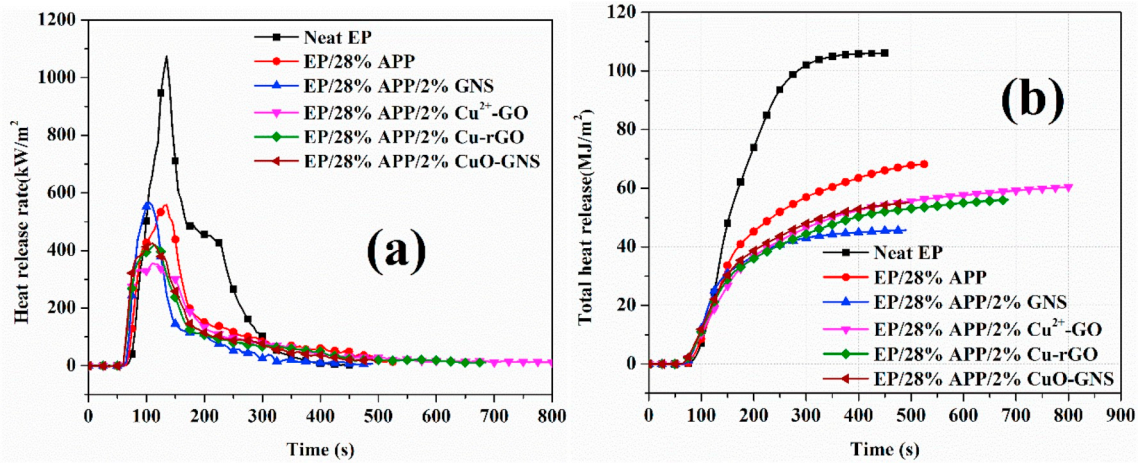

Fig. 8. HRR (a) and THR (b) curves of neat EP and EP composites with 28 wt% of flame retardants.

The lattice structures of GY100, GNS, Cu^{2+}-GO, Cu-rGO and CuO-GNS were investigated by XRD. As shown in Fig. 3, the XRD pattern of GY100 displays an intense peak at 10.82°, which corresponds to (002) plane. After exfoliation and reduction, the (002) peak of GNS moves to 26.35°, indicating that oxygen-containing groups have been removed from GY100 surface. For hybrids, the diffraction peaks of GY100 and GNS are severely weakened by the strong intensity of Cu compounds. Two sharp diffraction peaks of Cu-rGO at 43.28° and 50.43° are assigned to (111) and (200) crystal planes of Cu (JCPDS NO.04-0836), declaring that Cu^{2+} is reduced to Cu. In addition, the strong diffraction peaks of CuO-GNS at 32.52°, 35.53°, 38.68°, 48.69°, 53.47°, 58.26°, 61.52°, 66.20° and 68.12° belong to the (110), (−111), (111), (−202), (020), (202), (−113), (−311) and (220) planes of CuO (JCPDS NO.45-1548). Although the XRD pattern of Cu^{2+}-GO is similar to CuO-GNS, the characteristic peaks are different in intensity and degree. It illustrates that Cu^{2+}-GO and CuO-GNS have the different chemical structures, but their lattice structures may be similar.

To further demonstrate whether Cu^{2+}, Cu and CuO were successfully loaded on the graphene surface, the morphology of Cu^{2+}-GO, Cu-rGO and CuO-GNS are investigated by TEM. As shown in Fig. 4(a–c), GO, rGO and GNS sheets exhibit a typical crumpled carbon layer and a paper-like structure with thin layers, and large number of dark particles (Cu^{2+},

Table 3
The data of cone calorimeter test on neat EP and EP composites with 28 wt% of flame retardants.[a].

Sample	TTI (s)	PHRR (kW/m^2)	A_VHRR (kW/m^2)	t_P (s)	FIGRA	THR (MJ/m^2)	TSP (m^2)	AvEHC (MJ/kg)	CY (%)
Neat EP	62 ± 2	1075 ± 35	262 ± 14	135 ± 5	8.0	106 ± 5	51.6 ± 4.5	21.1 ± 0.1	5 ± 2
EP/28%APP	62 ± 1	558 ± 26	163 ± 19	135 ± 10	4.1	68 ± 8	27.6 ± 3.1	24.8 ± 0.3	38 ± 2
EP/28%APP/2%GNS	59 ± 3	567 ± 23	112 ± 15	105 ± 10	5.4	46 ± 7	27.8 ± 2.1	16.9 ± 0.2	40 ± 3
EP/28%APP/2%Cu^{2+}-GO	56 ± 4	355 ± 32	133 ± 13	110 ± 10	3.2	60 ± 3	26.1 ± 1.5	22.7 ± 0.4	43 ± 2
EP/28%APP/2%Cu-rGO	55 ± 3	418 ± 40	128 ± 15	115 ± 10	3.6	56 ± 3	25.7 ± 1.5	17.2 ± 0.3	41 ± 4
EP/28%APP/2%CuO-GNS	59 ± 3	380 ± 22	133 ± 12	130 ± 10	2.9	55 ± 4	23.0 ± 1.4	26.2 ± 0.5	41 ± 1

[a] TTI means time to ignition, PHRR represents peak of heat release rate, AvHRR is average heat release rate between 50 s and 450 s, t_P denotes time to PHRR, FIGRA is calculated by dividing the PHRR by T_p, THR represents total heat release, and AvEHC denotes average effective heat combustion between 50 s and 450 s, CY represents char yield.

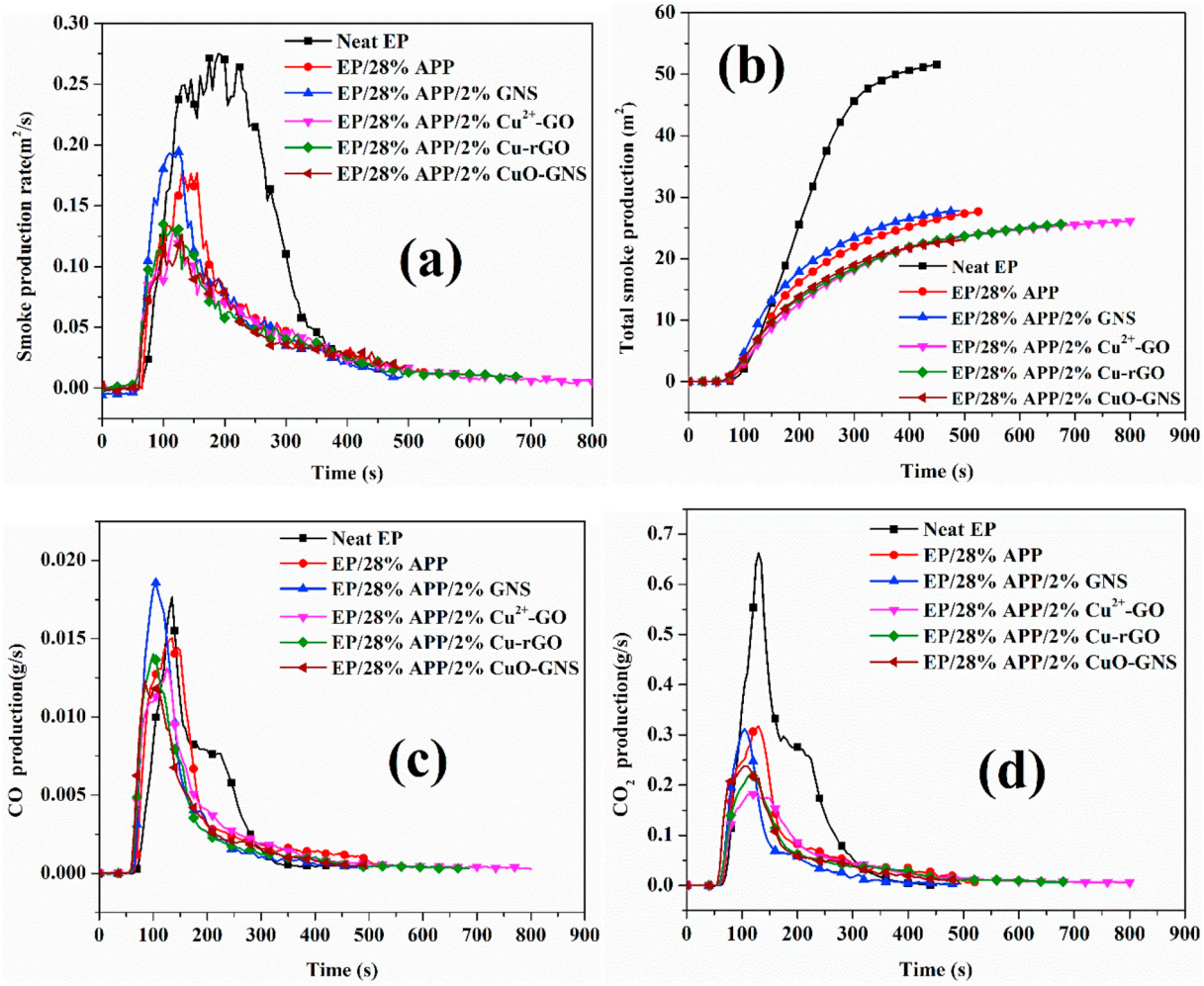

Fig. 9. SPR (a), TSP (b), COP (c), and CO_2P (d) curves of neat EP and EP composites with 28 wt% of flame retardants.

Cu and CuO) distribute on the sheets surface. Fig. 4 (a′-c′) show that the spacing between the lattice fringes of Cu^{2+}-GO, Cu-rGO and CuO-GNS are 0.24 nm, 0.20 nm and 0.26 nm, respectively. They are approximately equal to their calculated interplanar spacings according to the Bragg formula, 0.233 nm for Cu^{2+}-GO at 38.71° (111), 0.209 nm for Cu-rGO at 43.28° (111), and 0.253 nm for CuO-GNS at 35.50° (002). It confirms that Cu^{2+}, Cu and CuO are successfully located at graphene sheets as expected.

TGA was employed to evaluate the thermal stability of hybrids. The TG and DTG curves are shown in Fig. 5, and the data are listed in Table 1. From Fig. 5 (a) and (b), it can be seen clearly that the onset decomposition temperature ($T_{5\%}$), the maximum weight loss temperature (T_{max}) and char residue of GNS and hybrids are higher than those of GY100. Compared with GY100 and Cu^{2+}-GO, GNS, Cu-rGO and CuO-GNS are more stable, for the significant reduction of labile oxygen-containing groups in them. However, the heat resistance of oxygen-containing groups can be enhanced through the combination of Cu^{2+}.

To study the stability of Cu-rGO at the curing temperature of 80 °C for 2 h and 120 °C for 2 h, and to analyze the changes of hybrids' lattice structure before and after decompostion, these behaviors were investigated by XRD. As shown in Fig. 5 (c), only a minority of Cu and Cu-rGO are oxidized into Cu(II). It illustrates that Cu-rGO can hardly be oxidized under the curing conditions, especially dispersion in the epoxy matrix. Furthermore, there is still a small quantity of Cu-rGO are oxidized into Cu_2O and CuO as shown in Fig. 5 (d), when it was heated to 700 °C in nitrogen atmosphere. However, Cu^{2+}-GO is easy to be transferred into

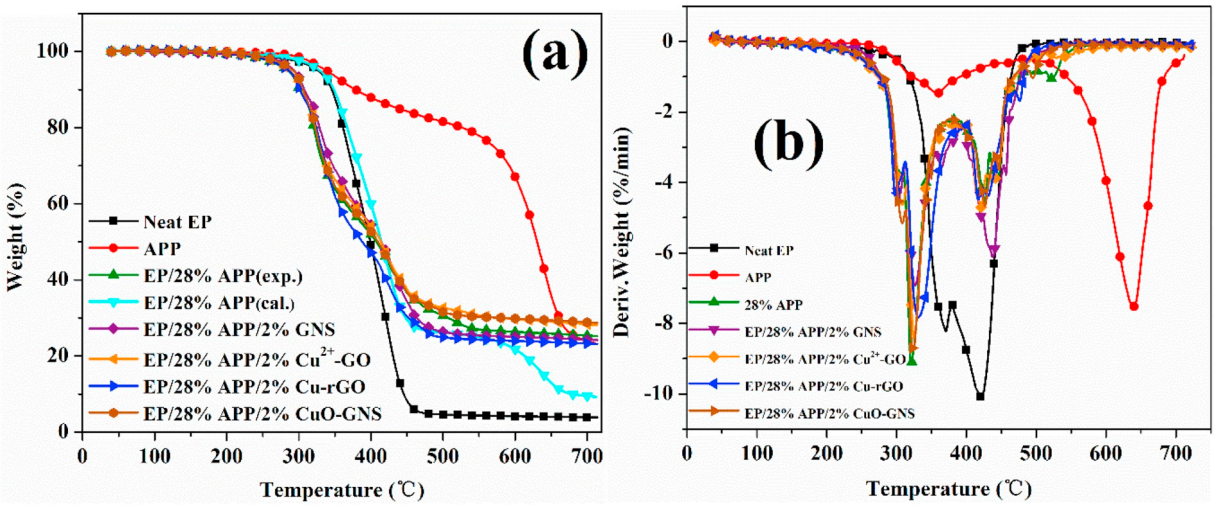

Fig. 10. TG (a) and DTG (b) curves of neat EP, and EP composites with 28 wt% of flame retardants at the heating rate of 10 °C/min in N_2.

Table 4
TGA data of neat EP, and EP composites with 28 wt% of flame retardants at the heating rate of 10 °C/min in N_2.[a]

Sample	$T_{1\%}$ (°C)	$R_{1\%}$ (%/min)	T_{max1} (°C)	R_{max1} (%/min)	T_{max2} (°C)	R_{max2} (%/min)	wt_R^{700} (%)
Neat EP	241	0.17	371	8.22	421	10.09	4
APP	289	0.35	357	1.48	639	7.53	24
EP/28%APP	219	0.21	321	9.12	427	4.52	25
EP/28%APP/2%GNS	224	0.17	327	6.89	438	6.09	24
EP/28%APP/2%Cu^{2+}-GO	236	0.36	324	8.40	421	4.70	28
EP/28%APP/2%Cu-rGO	226	0.28	332	7.83	432	4.58	23
EP/28%APP/2%CuO-GNS	238	0.29	324	8.77	427	4.67	29

[a] $T_{1\%}$ denotes the temperature at 1% weight loss; $R_{1\%}$ means mass loss rate at $T_{1\%}$.

Cu, Cu_2O and CuO through thermal redox reaction, since it contains a large number of oxygen-containing groups. CuO-GNS fails to be decomposed into other copper compounds under this condition. It indicates that Cu^{2+} is easier than Cu and CuO to go through various oxidation states and intermediates.

3.2. Morphology of EP composites

To determine the dispersion and compatibility of GNS and graphene hybrids, the microcosmic morphology change of EP composites is investigated by SEM. In Fig. 6 (a), the arrow marked particle is the dispersed phase, the circled area represents continuous phase. It shows clearly that rod-shaped APP particles (Fig. 6 a′) are evenly distributed throughout the matrix, but its compatibility with epoxy resin is poor. The compatibility can be obviously improved by the additon of extra hybrids (Cu^{2+}-GO, Cu-rGO and CuO-GNS) as displayed in Fig. 6(b–d). In addition, Cu^{2+}-GO exhibits better enhancement on compatibility than Cu-rGO and CuO-GNS, since the fracture surface of EP/APP/Cu^{2+}-GO has better continuity. It may be because the formation of hydrogen bonds between the oxygen-containing groups of Cu^{2+}-GO and the chains of epoxy resin. The hydrogen bonds cause Cu^{2+}-GO easier to agglomerate than Cu-rGO and CuO-GNS, shown in Fig. 6 (b′-d’).

3.3. Flammability of EP composites

The flame retardancy of cured EPs was evaluated via LOI and UL-94 vertical burning tests, the corresponding data are listed in Table 2, the digital photos of UL-94 test are displayed in Fig. 7. Obviously, pure EP is a very flammable material due to its low LOI value (20%), fast fire spread, and fire dripping. By addition of 28 wt% APP, the LOI value of EP/28%APP composite is significantly increased to 35.5%, but it still unable to reach UL-94 V-0 rating because it fails to restrain the fire spread and dripping after the second ignition. To achieve UL-94 V-0 rating, the minimum demand of APP reaches up to 30 wt%. UL-94 V-0 and higher LOI values can be obtained by adding 2 wt% extra synergists (GNS, Cu^{2+}-GO, Cu-rGO and CuO-GNS) in EP/28%APP system. In addition, hybrids have better synergistic effect than GNS on improving the flame-retardant efficiency of APP. On controlling the mass ratio of APP to hybrids as 14:1, the minimum loading of APP to get V-0 can be further reduced to 16.80 wt%, 21.47 wt% and 20.53 wt%, respectively, for EP/APP/Cu^{2+}-GO, EP/APP/Cu-rGO, and EP/APP/CuO-GNS. Obviously, Cu^{2+}-GO is the most effective one. Fig. 7 shows that Cu^{2+}-GO and other hybrids promote the carbonization rate, as well as prevent the fire spread and dripping. It probably due to the fact that these hybrids accelerate the crosslinking of pyrolytic viscous liquid and transfer it into char. Therefore, all the hybrids have significant synergistic effect with APP on enhancing char formation, and different oxidation state of copper and its compound structure result in different synergistic flame-retardant efficiency with APP.

To further study the synergistic flame-retardant behaviour, cone calorimeter measurement was utilized to assess the heat release, smoke production and toxic gases production of EP composites. The heat release rate (HRR) and total heat release (THR) curves are displayed in Fig. 8, the collected data are presented in Table 3. As shown in Fig. 8 (a), the HRR of neat EP sharply increases to peak value of 1075 kW/m^2 after being ignited. The peak of HRR (PHRR) can be distinctly declined to 558 kW/m^2 by loading of 28 wt% APP. In addition, it can be further reduced to 355 kW/m^2, 418 kW/m^2, 380 kW/m^2 by incorporating extra 2 wt% Cu^{2+}-GO, Cu-rGO and CuO-GNS in EP/28%APP, respectively. The incorporation of 2 wt% GNS fails to decrease the PHRR of EP/28% APP, however, GNS is better than Cu^{2+}-GO, Cu-rGO and CuO-GNS on reducing the AvHRR of EP/28%APP. It is owing to that GNS lacks in the catalytic action of copper ion or oxide, which can promote EP/APP rapid formation of an intumescent protective char layer. Besides, Cu^{2+}-GO has

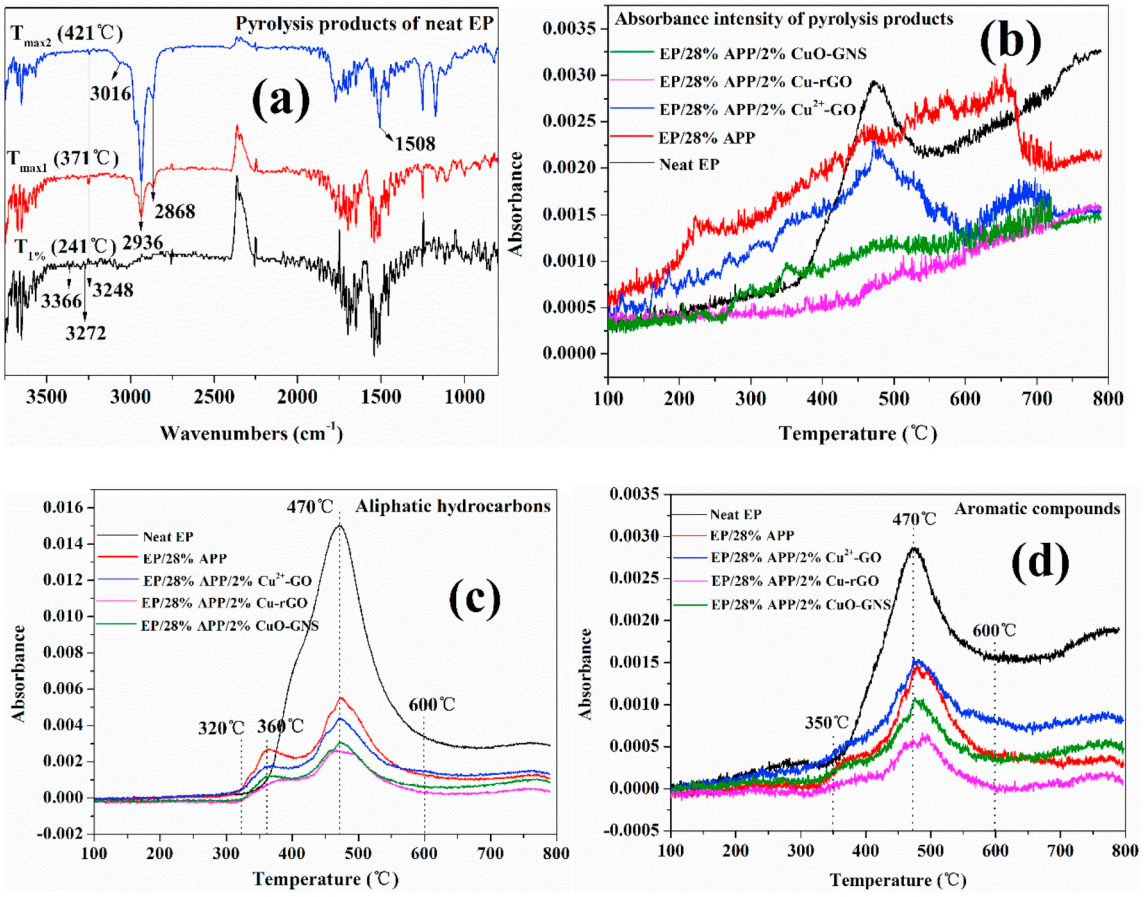

Fig. 11. FTIR spectra of pyrolysis products from neat EP (a), and the absorbance intensity of pyrolysis products (b), hydrocarbons (c) and aromatic compounds (d).

better synergistic effect with APP than Cu-rGO and CuO-GNS on decreasing the PHRR of EP/APP. This maybe because Cu^{2+} exhibits better catalytic carbonization as a Lewis acid than Cu and CuO.

Fig. 8 (b) shows that THR of EP/APP and its synergistic systems are also decreased dramatically because of high char yield (CY). Moreover, the variation of average effective heat combustion (AvEHC) indicates that the addition of APP and synergists change the types and contents of pyrolysis gases from EP. It is the interaction of the pyrolysis products that makes epoxy resins exhibit excellent flame-retardant performances.

Fire growth rate (FIGRA), is defined as the ratio of PHRR value and the time to PHRR (t_P), which is introduced to assess the hazard of developing fires [35]. The lower the FIGRA value, the better the fire safty of materials. Table 3 shows that the FIGRA value of neat EP is up to 8.0, which is much higher than that of EP/28%APP (4.1). It indicates that the presence of APP can significantly reduce the fire hazard of EP. In addition, the fire safety can be further improved by addition extra hybrids except GNS in EP/APP. This also demonstrates that Cu^{2+}-GO, Cu-rGO and CuO-GNS have excellent synergistic effect with APP on enhancing the flame retardancy of EP.

Most fire deaths are caused by smoke inhalation, oxygen deprivation, and toxic gases rather than burns [36]. EP has the critical defects of high flammability, dense smoke and poisonous gases. Therefore, SPR, TSP, CO production (COP) and CO_2 production (CO_2P) are important parameters to assess the fire hazard of EP. As shown in Fig. 9, the presence of APP can significantly decrease not only SPR and TSP, but COP and CO_2P. Besides, they can be further reduced by incorporation of extra Cu^{2+}-GO, Cu-rGO and CuO-GNS except GNS. This is because GNS lacks the catalytic power of copper. Compared to EP/28%APP, the TSP and COP values can be further lessened by 17% and 19%, respectively, by loading of 2 wt% CuO-GNS. CuO-GNS exhibits better synergistic effect with APP on smoke suppression and toxic gases reduction than the other two. It may be attributed to the fact that CuO-GNS plays a better role than Cu^{2+}-GO and Cu-rGO in conversion of CO to CO_2 through a redox cycle, involving the reduction of Cu^{2+}-Cu^{+}-Cu^{0} by CO and the oxidation of Cu^{0}–Cu^{+}-Cu^{2+} by O_2, according to our previous work [18].

3.4. Thermal decomposition behavior

TGA was employed to investigate the thermal decomposition behaviors of APP, neat EP and flame-retardant EP composites. In addition, the theoretical curve of EP/28%APP was calculated by the TG curves of APP and neat EP. TG and DTG curves of them are presented in Fig. 10, and the detailed data are listed in Table 4. Fig. 10 shows that all the samples have two dominating weight loss stages. As for virgin EP, thermal decomposition starts from 241 °C, chain scission begins to take place in large numbers at about 371 °C and the mass loss rate reaches its maximum (10.09%/min) at 421 °C. The dehydration of the secondary alcohol and the cleavage of polyamide chain is responsible for the onset decomposition and the first mass loss process. Meanwhile, the decomposition is accompanied by the generation of combustible gases, such as allyl alcohol, acetone and various hydrocarbons. At higher temperatures, the breakage of ether bond and biphenol A chain leads to the formation of polyaromatic hydrocarbons, such as naphthalene and phenanthrene, through pyro-synthesis and aromatization reactions [37]. For the absence of promoter for char formation, only 4% char residue remains in neat EP. The initial decomposition and the first mass loss process of APP result from the elimination of NH_3 and H_2O, and the primary weight loss occurs at higher temperature (around 639 °C). However, the presence of APP in EP results in the decrease of $T_{1\%}$, T_{max1} and R_{max2}, as well as the increase of R_{max1} and T_{max2}. The reason is that some interactions have been taken place between EP and APP. It also can be illustrated by the calculated TG curve. Especially, the pyrolysis

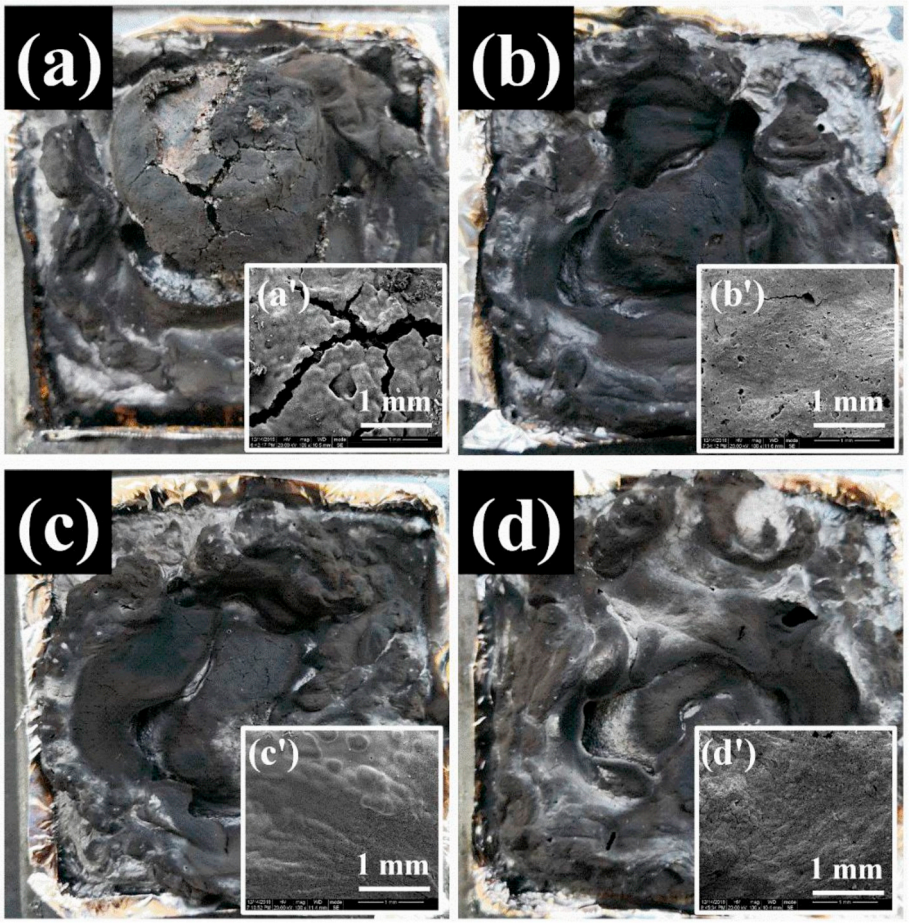

Fig. 12. Digital photos of char residue (a-d) and its microphotographs of external surface (a'-d') of EP/28%APP (a, a'), EP/28%APP/2%Cu^{2+}-GO (b, b'), EP/28% APP/2%Cu-rGO (c, c'), EP/28%APP/2%CuO-GNS (d, d').

products of APP, such as polyphosphoric acid derivatives, can accelerate the decomposition of EP at low temperature (321 °C) and promote the formation of protective char layer by catalytic dehydration. In addition, the formation of char can hinder the decomposition of EP at high temperature (427 °C) and increase the char residue yield to 25%.

Interestingly, with the addition of extra 2 wt% synergists, the $T_{1\%}$ and $R_{1\%}$ of EP/28%APP composites are increased considerably. Because the physical barrier of graphene, as well as the catalytic action of Cu^{2+}, Cu and CuO, contribute to the production of stable char residue earlier than APP alone in EP. The decrease in mass loss rate is the result of rapid carbonization of hybrid system. In addition, Cu^{2+}-GO and CuO-GNS containing EP/APP composites have higher char residues than that of EP/APP/Cu-rGO. It indicates that Cu^{2+}-GO and CuO-GNS have better synergistic effect than Cu-rGO on fixing carbon to reduce the production of flammable gases and to form phosphorus-rich residues.

3.5. Analysis of evolved gases

To study the composition and intensity of pyrolysis products, TGA coupled with FTIR was used to analyze the gases evolved from neat EP and EP composites. Fig. 11 (a) shows that the characteristic absorption peaks at 3366 cm^{-1}, 3272 cm^{-1} and 3248 cm^{-1} illustrate that the initial decomposition products of neat EP primarily consist of water and alcohols. The strong signals at 2936 cm^{-1} and 2868 cm^{-1} suggest that aliphatic hydrocarbons are the main pyrolysis gases at the first maximum weight loss stage. The pyrolysis gases at the second maximum weight loss stage contain not only aliphatic hydrocarbons but aromatic compounds (3016 cm^{-1} and 1508 cm^{-1}). It indicates that aliphatic hydrocarbons and aromatic compounds are the main components of smoke and harmful gases. As shown in Fig. 11 (b), the absorbance of pyrolysis products can be decreased by addition of APP in EP, and it can be further reduced by loading with extra 2 wt% hybrids, especially the addition of Cu-rGO and CuO-GNS. It may be due to the fact that Cu^{2+} is easier than Cu and CuO to go through various oxidation states and intermediates, which tend to catalyze both the breakage and formation of C–C bonds, before reaching final oxide state. This catalytic action is beneficial to form polyaromatic char in the condensed phase and hydrocarbons in the gaseous phase, such as naphthalene and phenanthrene. In addition, Fig. 11 (c) and (d) display that the combination of hybrids with APP can also further reduce the maximum absorbance intensity of aliphatic hydrocarbons and aromatic compounds. Lower absorbance means lower concentration of smoke. The generation of aliphatic hydrocarbons is earlier than aromatic compounds, and both of them reach the peak value at 470 °C and stop at 600 °C. This indicates that the decomposition of EP is related to its chain structure, specifically, it depends on the thermal stabilities of monomers, crosslinking densities of resin, and the effects of additives. Here, the aliphatic hydrocarbons may be firstly produced from polyamide chain, and the aromatic compounds are primarily generated from biphenol A chain. Besides, the loading of APP and hybrids leads to the appearance of new absorbance peaks at 360 °C, compared to neat EP. This suggests that both APP and hybrids accelerate the decomposition of EP at low temperature and promote the formation of protective char layer, which hinder the further decomposition of matrix. As a result, smoke and harmful gases are significantly reduced.

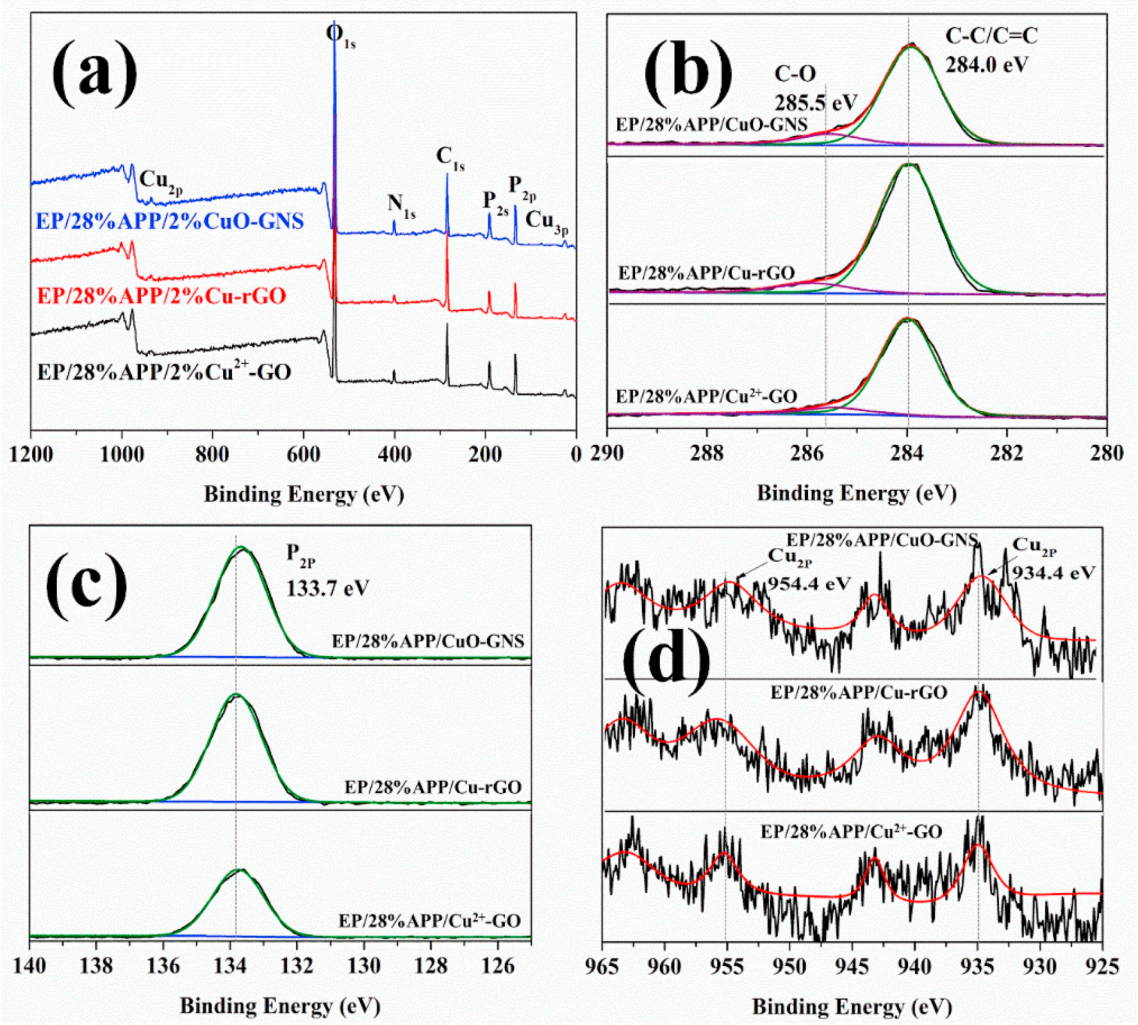

Fig. 13. XPS spectra of all elements (a), C_{1s} (b), P_{2p} (c) and Cu_{2p} (d) of the char residue of EP/28%APP/2%Cu^{2+}-GO, EP/28%APP/2%Cu-rGO, EP/28%APP/2% CuO-GNS.

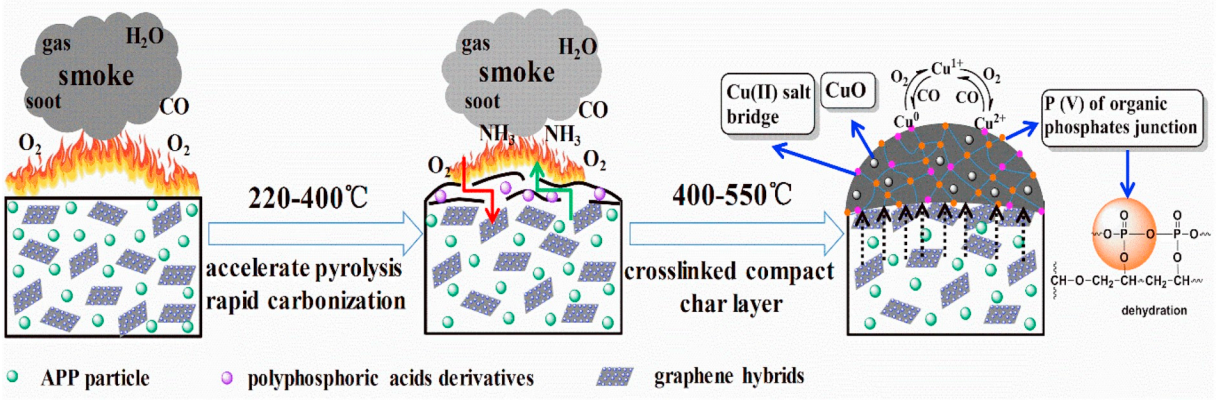

Fig. 14. The model of flame-retardant mechanism for EP/APP composites containing graphene hybrids.

3.6. Analysis of residual chars

To investigate the effect of hybrids on the char formation of EP/APP composite, the microstructure and composition of chars obtained from cone calorimeter test were examined by SEM and XPS. Fig. 12 shows the digital photos and external char morphologies of EP composites. Some cracks are observed on the external surface of EP/28%APP char, but a compact char layer is obtained by adding hybrids in EP/APP system. This implies that the physical barrier of graphene, as well as the catalytic action of hybrids are helpful to enhance the compactness and strength of char.

Fig. 13 displays the XPS spectra of char residues from EP/APP containing hybrids. Fig. 13 (a) shows that carbon-, oxygen-, phosphorus-, nitrogen-, and copper-containing groups are found to accumulate in char

residues. As shown in Fig. 13 (b), the strong peak of char residue at 284.0 eV and weak peak at 285.5 eV are assigned to C–C/C=C and C–O bonds of C_{1s} spectrum, respectively. It illustrates that the char residue is a graphitized structure containing polyaromatic rings. The P_{2p} peak at 133.7 eV (Fig. 13 c) indicates that final oxidation state of phosphorus in the char is P (V) of organic phosphates, which can act as the junction and bridge of crosslinking char. In addition, as shown in Fig. 13 (d), the Cu_{2p} peaks at 934.4 eV and 954.4 eV suggest that the final oxidation state of copper in the char is Cu (II) of oxides, salts or complexes, which may act as not only salt bridge for crosslinking but reinforcing agent for char layer. Therefore, Cu^{2+}-GO, Cu-rGO and CuO-GNS have excellent synergistic effect with APP on improving the formation rate, amount and compactness of char.

According to the analysis of decomposition behaviors and pyrolysis products, the model of flame-retardant mechanism for EP/APP composites containing graphene hybrids is proposed in Fig. 14. It can be summerized as follows: (i) graphene hybrids further accelerate the decomposition of EP/APP composite at low temperature (220–400 °C), resulting in the increase of carbonization rate, which is benificial to produce stable char earlier than EP/APP composite. Rapid carbonization tends to restrain fire spread and dripping. (ii) A compact char layer is formed before 550 °C by increasing the crosslinking junctions of chars with P (V) organic phosphates and Cu (II) salts. The compact char layer is a good barrier to heat, air/O_2 and pyrolysis products. (iii) Cu (II) decorated grahene is better than Cu(0) decorated graphene on fixing carbon and oxidating CO. This contributes to the reduction of smoke and harmful gases, such as aliphatic hydrocarbons, aromatic compounds and CO.

4. Conclusion

Three graphene hybrids, which were attached with diverse forms of cupric compounds (Cu^{2+}, Cu, CuO), were successfully synthesized through benign methods. All the hybrids (Cu^{2+}-GO, Cu-rGO and CuO-GNS) have siginificant synergistic effect with APP on enhancing the flame retardancy of EP, and the different oxidation state of copper and its chemical structure result in different synergistic efficiency with APP. Specifically, Cu^{2+}-GO exhibits better synergistic effect on enhancing flame retardancy, but CuO-GNS exhibits better on smoke and toxic gases reduction. In addition, the final oxidation state of copper in the char is Cu (II) of oxides, salts or complexes, which may act as not only salt bridge for crosslinking but reinforcing agent for the phosphorus-rich char.

Acknowledgment

This work was financially supported by the National Natural Science Foundation of China (21504071), and the Key Project of Sichuan Provincial Department of Education (16ZA0159).

References

[1] Schmidt C, Ciesielski M, Greiner L, Döring M. Novel organophosphorus flame retardants and their synergistic application in novolac epoxy resin. Polym Degrad Stab 2018;158:190–201.
[2] Jian R, Wang P, Duan W, Wang J, Zheng X, Weng J. Synthesis of a novel P/N/S-containing flame retardant and its application in epoxy resin: thermal property, flame retardance, and pyrolysis behavior. Ind Eng Chem Res 2016;55:11520–7.
[3] Morgan AB. The future of flame retardant polymers – unmet needs and likely new approaches. Polym Rev 2018:1–30. https://doi.org/10.1080/15583724.2018.1454948.
[4] Wang L, Yang W, Wang B, Wu Y, Hu Y, Song L, Yuen RKK. The impact of metal oxides on the combustion behavior of ethylene–vinyl acetate coploymers containing an intumenscent flame retardant. Ind Eng Chem Res 2012;51:7884–90.
[5] Tan Y, Shao ZB, Yu LX, Long JW, Qi M, Chen L, Wang YZ. Piperazine-modified ammonium polyphosphate as monocomponent flame-retardant hardener for epoxy resin: flame retardance, curing behavior and mechanical property. Polym Chem 2016;7:3003–12.
[6] Bourbigot S, Le Bras M, Dabrowski F, Gilman JW, Kashiwagi T. PA-6 clay nanocomposite hybrid as char rorming agent in intumescent formulations. Fire Mater 2000;24:201–8.
[7] Wang JS, Wang DY, Liu Y, Ge XG, Wang YZ. Polyamide-enhanced flame retardancy of ammonium polyphosphate on epoxy resin. J Appl Polym Sci 2008;108:2644–53.
[8] Zhang W, He X, Song T, Jiao Q, Yang R. Comparison of intumescence mechanism and blowing-out effect in flame-retarded epoxy resins. Polym Degrad Stab 2015;112:43–51.
[9] Li B. A study of the thermal decomposition and smoke suppression of poly(vinyl chloride) treated with metal oxides using a cone calorimeter at a high incident heat flux. Polym Degrad Stab 2002;78:349–56.
[10] Kicko-Walczak E, Rymarz G. Recent developments in fire-retardant thermoset resins using inorganic-organic hybrid flame retardants. J Polym Eng 2018;38:563–71.
[11] Qiu S, Xing W, Feng X, Yu B, Mu X, Yuen RKK, Hu Y. Self-standing cuprous oxide nanoparticles on silica@ polyphosphazene nanospheres: 3D nanostructure for enhancing the flame retardancy and toxic effluents elimination of epoxy resins via synergistic catalytic effect. Chem Eng J 2017;309:802–14.
[12] Zou XP, Wang LN, Li XN, Liu QY, Zhao YX, Ma TM, He SG. Noble-metal-free single-atom catalysts $CuAl4O_{7-9}$ for CO oxidation by O_2. Angew Chem Int Ed 2018;57:10989–93.
[13] Wang LN, Li XN, Jiang LX, Yang B, Liu QY, Xu HG, Zheng WJ, He SG. Catalytic CO oxidation by O_2 mediated by noble-metal-free cluster anions Cu_2VO_{3-5}. Angew Chem Int Ed 2018;57:3349–53.
[14] Jia AP, Hu GS, Meng L, Xie YL, Lu JQ, Luo MF. CO oxidation over CuO/$Ce_{1-x}Cu_xO_{2-\delta}$ and $Ce_{1-x}Cu_xO_{2-\delta}$ catalysts: synergetic effects and kinetic study. J Catal 2012;289:199–209.
[15] Naik AD, Bourbigot S, Bellayer S, Touati N, Ben Tayeb K, Vezin H, Fontaine G. Salen complexes as fire protective agents for thermoplastic polyurethane: deep electron paramagnetic resonance spectroscopy investigation. ACS Appl Mater Inter 2018;10:24860–75.
[16] Liu L, Qian M, Song P, Huang G, Yu Y, Fu S. Fabrication of green lignin-based flame retardants for enhancing the thermal and fire retardancy properties of polypropylene/wood composites. ACS Sustain Chem Eng 2016;4:2422–31.
[17] White B, Yin M, Hall A, Le D, Stolbov S, Rahman T, Turro N, O'Brien S. Complete CO oxidation over Cu_2O nanoparticles supported on silica gel. Nano Lett 2006;6:2095–8.
[18] Chen MJ, Lin YC, Wang XN, Zhong L, Li QL, Liu ZG. Influence of cuprous oxide on enhancing the flame retardancy and smoke suppression of epoxy resins containing microencapsulated ammonium polyphosphate. Ind Eng Chem Res 2015;54:12705–13.
[19] Chen MJ, Wang X, Li XL, Liu XY, Zhong L, Wang HZ, Liu ZG. The synergistic effect of cuprous oxide on an intumescent flame-retardant epoxy resin system. RSC Adv 2017;7:35619–28.
[20] Chen D, Feng H, Li J. Graphene oxide: preparation, functionalization, and electrochemical applications. Chem Rev 2012;112:6027–53.
[21] Dreyer DR, Park S, Bielawski CW, Ruoff RS. The chemistry of graphene oxide. Chem Soc Rev 2010;39:228–40.
[22] Fang F, Ran S, Fang Z, Song P, Wang H. Improved flame resistance and thermo-mechanical properties of epoxy resin nanocomposites from functionalized graphene oxide via self-assembly in water. Compos Part B 2019;165:406–16.
[23] Kim MJ, Jeon IY, Seo JM, Dai L, Baek JB. Graphene phosphonic acid as an efficient flame retardant. ACS Nano 2014;8:2820–5.
[24] Daud M, Kamal MS, Shehzad F, Al-Harthi MA. Graphene/layered double hydroxides nanocomposites: a review of recent progress in synthesis and applications. Carbon 2016;104:241–52.
[25] Liu S, Yan H, Fang Z, Wang H. Effect of graphene nanosheets on morphology, thermal stability and flame retardancy of epoxy resin. Compos Sci Technol 2014;90:40–7.
[26] Liang Y, Li Y, Wang H, Zhou J, Wang J, Regier T, Dai H. Co_3O_4 nanocrystals on graphene as a synergistic catalyst for oxygen reduction reaction. Nat Mater 2011;10:780–6.
[27] Liu S, Fang Z, Yan H, Chevali VS, Wang H. Synergistic flame retardancy effect of graphene nanosheets and traditional retardants on epoxy resin. Compos Part A 2016;89:26–32.
[28] Heidar Pour R, Soheilmoghaddam M, Hassan A, Bourbigot S. Flammability and thermal properties of polycarbonate/acrylonitrile-butadiene-styrene nanocomposites reinforced with multilayer graphene. Polym Degrad Stab 2015;120:88–97.
[29] Nie H, Fu L, Zhu J, Yang W, Li D, Zhou L. Excellent tribological properties of lower reduced graphene oxide content copper composite by using a one-step reduction molecular-level mixing process. Materials 2018. https://doi.10.3390/ma11040600.
[30] Li Z, González AJ, Heeralal VB, Wang DY. Covalent assembly of MCM-41 nanospheres on graphene oxide for improving fire retardancy and mechanical property of epoxy resin. Compos Part B 2018;138:101–12.
[31] Shi Y, Qian X, Zhou K, Tang Q, Jiang S, Wang B, Yu B, Hu Y, Yuen RKK. CuO/graphene nanohybrids: preparation and enhancement on thermal stability and smoke suppression of polypropylene. Ind Eng Chem Res 2013;52:13654–60.
[32] Wang D, Kan Y, Yu X, Liu J, Song L, Hu Y. In situ loading ultra-small Cu_2O nanoparticles on 2D hierarchical TiO_2-graphene oxide dual-nanosheets: towards reducing fire hazards of unsaturated polyester resin. J Hazard Mater 2016;320:504–12.
[33] Xu W, Zhang B, Wang X, Wang G, Ding D. The flame retardancy and smoke suppression effect of a hybrid containing $CuMoO_4$ modified reduced graphene oxide/layered double hydroxide on epoxy resin. J Hazard Mater 2018;343:364–75.

[34] Liu Y, Babu HV, Zhao J, Goñi-Urtiaga A, Sainz R, Ferritto R, Pita M, Wang DY. Effect of Cu-doped graphene on the flammability and thermal properties of epoxy composites. Compos Part B 2016;89:108–16.
[35] Schartel B, Hull TR. Development of fire-retarded materials-interpretation of cone calorimeter data. Fire Mater 2007;31:327–54.
[36] Irvine DJ, McCluskey JA, Robinson IM. Fire hazards and some common polymers. Polym Degrad Stab 2000;67:383–96.
[37] Levchik SV, Weil ED. Thermal decomposition, combustion and flame-retardancy of epoxy resins? a review of the recent literature. Polym Int 2004;53:1901–29.